Charm multiplicity and the branching ratios of inclusive charmless b quark decays in the general two-Higgs-doublet models

Zhenjun Xiao* and Chong Sheng Li

Department of Physics, Peking University, Beijing, 100871 People's Republic of China

Kuang-Ta Chao

CCAST (World Laboratory), P.O. Box 8730, Beijing 100080, People's Republic of China
and Department of Physics, Peking University, Beijing, 100871 People's Republic of China
(Received 13 March 2000; published 2 October 2000)

In the framework of general two-Higgs-doublet models, we calculate the branching ratios of various inclusive charmless b decays by using the low-energy effective Hamiltonian including next-to-leading order QCD corrections, and examine the current status and the new physics effects on the determination of the charm multiplicity n_c and semileptonic branching ratio B_{SL}. Within the considered parameter space, the enhancement to the ratio BR($b \to sg$) due to the charged-Higgs penguin diagrams can be as large as a factor of 8 (3) in the model III (II), while the ratio BR($b \to$ no charm) can be increased from the standard model prediction of 2.49 to 4.91 % (2.99%) in model III (II). Consequently, the value of B_{SL} and n_c can be decreased simultaneously in model III. The central value of B_{SL} will be lowered slightly by about 0.003, but the ratio n_c can be reduced significantly from the theoretical prediction of $n_c = 1.28 \pm 0.05$ in the SM to $n_c = 1.23 \pm 0.05$, 1.18 ± 0.05 for $m_{H^+} = 200$, 100 GeV, respectively. We find that the predicted n_c and the measured n_c now agree within roughly one standard deviation after taking into account the effects of gluonic charged Higgs penguin diagrams in model III with a relatively light charged Higgs boson.

PACS number(s): 13.25.Hw, 12.15.Ji, 12.38.Bx, 12.60.Fr

I. INTRODUCTION

In the forthcoming years, experiments at SLAC and KEK B factories, DESY HERA-B and other high-energy colliders will measure various branching ratios and CP-violating asymmetries of B decays [1,2]. The expected large number of B decay events (say $10^8 - 10^9$) may allow us to explore the physics of CP violation, to determine the flavor parameters of the electroweak theory, and to probe for signals or evidence of new physics beyond the standard model (SM) [1–6].

Among various B meson decay modes, the decays $b \to s\gamma$ and $b \to sg$ have been, for example, the hot subject of many investigations [7], since these decay modes may be affected by loop contributions from various new physics models. Great progress in both the theoretical calculation [8] and the experimental measurement [9] has enabled us to constrain the new physics models, such as the two-Higgs-doublet model (2HDM) [10], the minimal supersymmetric standard model [11] and the technicolor models [12].

For many years, it appeared that the SM prediction for the semileptonic branching ratio B_{SL} [13] was much larger than the values measured at Υ resonance and Z^0 peak [14,15]. More recently, the theoretical predictions have been refined by including full $O(\alpha_s)$ QCD corrections [16,17]. This progress, consequently, has lowered the predicted B_{SL} and now adequately reproduces the experimental results [15]. However, the measured values of B_{SL} at the $\Upsilon(4S)$ and Z^0 resonance are still lower slightly than the theoretical predictions [18]. In addition to the B_{SL} problem, there is another

so-called ''missing charm puzzle'' [15,19]: the charm multiplicity n_c measured at CLEO and the CERN e^+e^- collider LEP [18,20] (especially at CLEO, the Υ resonance) is smaller than the theoretical prediction. Among various possible explanations for the missing charm-B_{SL} problem, the most intriguing one is an enhanced $B \to X_{\text{no charm}}$ rate due to new physics beyond the SM [19]. An enhanced $b \to sg$ can decrease the values of both n_c and the B_{SL} simultaneously [19]. The large branching ratio BR($B \to \eta' X_s$) reported recently by CLEO [21] provided a new hint for enhanced $b \to sg$. In addition to those explanations based on the SM [22], new physics interpretations for this large ratio are also plausible [23].

In a previous paper [24], we calculated, from the first principles, the new contributions to inclusive charmless b quark decays $b \to sg, b \to sq\bar{q}$ from the gluonic charged-Higgs penguin diagrams in the so-called model III: the two-Higgs-doublet model (2HDM) with flavor changing couplings [25,26]. In the considered parameter space, we found that the branching ratio BR($b \to sg$) ($q^2 = 0$) can be increased by roughly an order of magnitude, which is much larger than that in the ordinary 2HDM's [27]. In Ref. [24], however, we used the language of form factors F_1 and F_2 and took into account the QCD corrections partially by using the $\alpha_s(m_b)$ directly to calculate the branching ratios.

In this paper, in the framework of general 2HDM's, we calculate the branching ratios of various inclusive charmless b decays by using the low energy effective Hamiltonian including next-to-leading order (NLO) QCD corrections [6], and investigate the new physics effects on the theoretical predictions for both B_{SL} and n_c.

This paper is organized as follows. In Sec. II, we describe the basic structures of model III, extract out the Wilson co-

---

*Email: zxiao@ibm320h.phy.pku.edu.cn

62 094008-1

efficients, draw the constraint on parameter space of model III from currently available data. In Sec. III, we calculate the branching ratios BR($b \to sg$) and BR($b \to q'q\bar{q}$) for $q' \in d,s$ and $q \in u,d,s$ in models III and II with the inclusion of NLO QCD corrections. In Sec. IV, we examine the current status and new physics effects on the determination of B_{SL} and n_c. The conclusions and discussions are included in the final section.

II. THE GENERAL 2HDM'S AND EXPERIMENTAL CONSTRAINT

The simplest extension of the SM is the so-called two-Higgs-doublet models [10]. In such models, the tree level flavor changing neutral currents (FCNC's) are absent if one introduces an *ad hoc* discrete symmetry to constrain the 2HDM scalar potential and Yukawa Lagrangian. Let us consider a Yukawa Lagrangian of the form [26]

$$\mathcal{L}_Y = \eta_{ij}^U \bar{Q}_{i,L} \tilde{\phi}_1 U_{j,R} + \eta_{ij}^D \bar{Q}_{i,L} \phi_1 D_{j,R} + \xi_{ij}^U \bar{Q}_{i,L} \tilde{\phi}_2 U_{j,R}$$
$$+ \xi_{ij}^D \bar{Q}_{i,L} \phi_2 D_{j,R} + \text{H.c.,} \qquad (1)$$

where ϕ_i ($i=1,2$) are the two Higgs doublets of a two-Higgs-doublet model, $\tilde{\phi}_{1,2} = i\tau_2 \phi_{1,2}^*$, $Q_{i,L}$ ($U_{j,R}$) with $i = (1,2,3)$ are the left-handed isodoublet quarks (right-handed up-type quarks), $D_{j,R}$ are the right-handed isosinglet down-type quarks, while $\eta_{i,j}^{U,D}$ and $\xi_{i,j}^{U,D}$ ($i,j=1,2,3$ are family index) are generally the nondiagonal matrices of the Yukawa coupling. By imposing the discrete symmetry

$$\phi_1 \to -\phi_1, \ \phi_2 \to \phi_2, \ D_i \to -D_i, \ U_i \to \mp U_i \qquad (2)$$

one obtains the so-called models I and II. In model I the third and fourth term in Eq. (1) will be dropped by the discrete symmetry, therefore, both the up- and down-type quarks get mass from Yukawa couplings to the same Higgs doublet ϕ_1, while the ϕ_2 has no Yukawa couplings to the quarks. For model II, on the other hand, the first and fourth term in Eq. (1) will be dropped by imposing the discrete symmetry. Model II has, consequently the up- and down-type quarks getting mass from Yukawa couplings to two different scalar doublets ϕ_1 and ϕ_2.

During past years, models I and II have been studied extensively in literature and tested experimentally, and model II has been very popular since it is the building block of the minimal supersymmetric standard model. In this paper, we focus on the third type of 2HDM [25], usually known as model III [25,26]. In model III, no discrete symmetry is imposed and both up- and down-type quarks then may have diagonal and/or flavor changing couplings with ϕ_1 and ϕ_2. As described in Ref. [26], one can choose a suitable basis ($H^0, H^1, H^2, H^\pm$) to express two Higgs doublets [26]

$$\phi_1 = \frac{1}{\sqrt{2}} \begin{pmatrix} \sqrt{2}\chi^+ \\ v+H^0+i\chi^0 \end{pmatrix}, \quad \phi_2 = \frac{1}{\sqrt{2}} \begin{pmatrix} \sqrt{2}H^+ \\ H^1+iH^2 \end{pmatrix}, \quad (3)$$

and take their vacuum expectation values as the form

$$\langle \phi_1 \rangle = \begin{pmatrix} 0 \\ v/\sqrt{2} \end{pmatrix}, \quad \langle \phi_2 \rangle = 0, \qquad (4)$$

where $v = (\sqrt{2}G_F)^{-1/2} = 246$ GeV. The transformation relation between (H^0, H^1, H^2) and the mass eigenstates ($\bar{H}^0, h^0, A^0$) can be found in Ref. [26]. The $H^\pm$ are the physical charged Higgs boson, H^0 and h^0 are the physical CP-even neutral Higgs boson and the A^0 is the physical CP-odd neutral Higgs boson. After the rotation of quark fields, the Yukawa Lagrangian of quarks are of the form [26]

$$\mathcal{L}_Y^{\text{III}} = \eta_{ij}^U \bar{Q}_{i,L} \tilde{\phi}_1 U_{j,R} + \eta_{ij}^D \bar{Q}_{i,L} \phi_1 D_{j,R} + \hat{\xi}_{ij}^U \bar{Q}_{i,L} \tilde{\phi}_2 U_{j,R}$$
$$+ \hat{\xi}_{ij}^D \bar{Q}_{i,L} \phi_2 D_{j,R} + \text{H.c.,} \qquad (5)$$

where $\eta_{ij}^{U,D}$ correspond to the diagonal mass matrices of up- and down-type quarks, while the neutral and charged flavor changing couplings will be [26][1]

$$\xi_{ij}^{U,D} = \frac{\sqrt{m_i m_j}}{v} \lambda_{ij}, \quad \hat{\xi}_{\text{neutral}}^{U,D} = \xi^{U,D},$$

$$\hat{\xi}_{\text{charged}}^U = \xi^U V_{\text{CKM}}, \quad \hat{\xi}_{\text{charged}}^D = V_{\text{CKM}} \xi^D, \qquad (6)$$

where V_{CKM} is the Cabibbo-Kobayashi-Maskawa mixing matrix [28], $i,j = (1,2,3)$ are the generation index. The coupling constants λ_{ij} are free parameters to be determined by experiments, and they may also be complex.

In model II and assuming $\tan\beta = 1$, the constraint on the mass of charged Higgs boson due to CLEO data of $b \to s\gamma$ is $M_{H^+} \geq 350$ (200) GeV at the LO (NLO) level [29,30]. For model I, however, the limit can be much weaker due to the possible destructive interference with the SM amplitude.

For model III, the situation is not as clear as model II because there are more free parameters here. As pointed in Ref. [26], the data of K^0-$\bar{K}^0$ and B_d^0-$\bar{B}_d^0$ mixing processes put severe constraint on the FC couplings involving the first generation of quarks. One therefore assumes that

$$\lambda_{uj} = \lambda_{dj} = 0, \quad \text{for } j = 1,2,3. \qquad (7)$$

Imposing the limit in Eq. (7) and assuming all other λ_{ij} parameters are of order 1, Atwood *et al.* [31] found a very strong constraint of $M_{H^+} > 600$ GeV by using the CLEO data of $b \to s\gamma$ decay available in 1995. In Ref. [32], Aliev *et al.* studied the $b \to s\gamma$ decay in model III by extending the NLO results of model II [30] to the case of model III, and found some constraints on the FC couplings.

---

[1]We make the same ansatz on the $\xi_{ij}^{U,D}$ couplings as the Ref. [26]. For more details about the definition of $\hat{\xi}^{U,D}$ one can see Ref. [26].

In a recent paper [33], Chao *et al.*, studied the decay $b \to s\gamma$ by assuming that only the couplings λ_{tt} and λ_{bb} are nonzero. They found that the constraint on M_{H^+} imposed by the CLEO data of $b \to s\gamma$ can be greatly relaxed by considering the phase effects of λ_{tt} and λ_{bb}. The constraints by B^0-$\bar{B}^0$ mixing, the neutron electric dipole moment (NEDM), the Z^0-pole parameter ρ and R_b give the following preferred scenario [33]:

$$|\lambda_{tt}| \leq 0.3, \quad |\lambda_{bb}| \approx 50, \quad M_{A^0} \approx M_{h^0} = 80 - 120 \ \text{GeV};$$

$$80 \ \text{GeV} \leq M_{H^+} \leq 200 \ \text{GeV}. \tag{8}$$

In the following sections, we will calculate the new physics contributions to the inclusive charmless decays of b quark in the Chao-Cheung-Keung (CCK) scenario of model III [33]. Model III has the following advantages.

(1) Since we keep only the couplings λ_{tt} and λ_{bb} nonzero, the neutral Higgs bosons do not contribute at tree level or one-loop level. The new contributions therefore come only from the charged Higgs penguin diagrams with the heavy internal top quark.

(2) The new operators $O_{9,10}$ and all flipped chirality partners of operators $O_{1,\ldots,10}$ as defined in Ref. [32] do not contribute to the decay $b \to s\gamma$ and other inclusive charmless decays under study in this paper.

(3) The free parameters in model III are greatly reduced to λ_{tt}, λ_{bb}, and M_{H^+}.

In order to find more details about the correlations between M_{H^+} and couplings $\lambda_{tt,bb}$ by imposing the new CLEO data of $b \to s\gamma$, we recalculate the decay $b \to s\gamma$ in model III. For the sake of simplicity, we do not consider the less interesting model I further in this paper.

The effective Hamiltonian for $B \to X_S \gamma$ at the scale $\mu = O(m_b)$ is given by [4]

$$\mathcal{H}_{\text{eff}}(b \to s\gamma)$$

$$= -\frac{G_F}{\sqrt{2}} V_{ts}^* V_{tb}$$

$$\times \left[\sum_{i=1}^{6} C_i(\mu) Q_i(\mu) + C_{7\gamma}(\mu) Q_{7\gamma} + C_{8G}(\mu) Q_{8G} \right]. \tag{9}$$

The explicit expressions of operators $Q_{1-6}, Q_{7\gamma}$ and Q_{8G}, as well as the corresponding Wilson coefficients $C_i(M_W)$ in the SM can be found, for example, in Ref. [4].

In model III, the left-handed QED magnetic-penguin operator $Q_{7\gamma}^L$ and the left-handed QCD magnetic-penguin operator Q_{8G}^L may also play an important role:

$$Q_{7\gamma}^L = \frac{e}{8\pi^2} m_b \bar{s}_\alpha \sigma^{\mu\nu} (1 - \gamma_5) b_\alpha F_{\mu\nu}, \tag{10}$$

$$Q_{8G}^L = \frac{g_s}{8\pi^2} m_b \bar{s}_\alpha \sigma^{\mu\nu} (1 - \gamma_5) T_{\alpha\beta}^a b_\beta G_{\mu\nu}^a. \tag{11}$$
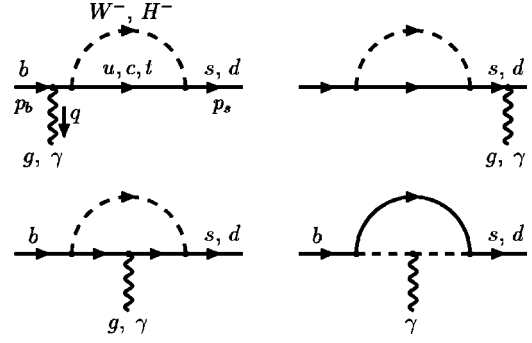

FIG. 1. The Feynman diagrams for the decays $b \to s\gamma$ and $b \to sg$ in the SM and 2HDM's. The internal quarks are the upper type u, c, and t quarks.

In the SM and ordinary 2HDM's, both operators $Q_{7\gamma}^L$ and Q_{8G}^L are absent because one usually assume that $m_s/m_b \sim 0$. In model III, however, these two left-handed operators may contribute effectively because the Wilson coefficients $C_{7\gamma}^L$ and C_{8G}^L may be rather large to compensate for the suppression of m_s/m_b.

In Ref. [24], we calculated the $b \to sg$ decay in model III from the first principle and obtained the corresponding form factors F_1 and F_2. Following the standard procedure and using the Feynman rules in model III [26], we evaluate the Feynman diagrams for both $b \to s\gamma$ and $b \to sg$ decay as shown in Fig. 1, extract out the Wilson coefficients $C_i(M_W)$ at the energy scale M_W by matching the full theory onto the effective theory

$$C_i(M_W) = 0 \quad (i = 1, 3, 4, 5, 6), \tag{12}$$

$$C_2(M_W) = 1, \tag{13}$$

$$C_{7\gamma}^L(M_W) = -\frac{m_s}{18 m_b} D(y_t) |\lambda_{tt}|^2, \tag{14}$$

$$C_{7\gamma}^R(M_W) = C_{7\gamma}(M_W)^{\text{SM}} - \frac{1}{12} A(y_t) |\lambda_{tt}|^2$$

$$+ \frac{1}{2} B(y_t) |\lambda_{tt} \lambda_{bb}| e^{i\theta}, \tag{15}$$

$$C_{8G}^L(M_W) = -\frac{m_s}{12 m_b} D(y_t) |\lambda_{tt}|^2, \tag{16}$$

$$C_{8G}^R(M_W) = C_{8G}(M_W)^{\text{SM}} - \frac{1}{12} D(y_t) |\lambda_{tt}|^2$$

$$+ \frac{1}{2} E(y_t) |\lambda_{tt} \lambda_{bb}| e^{i\theta}, \tag{17}$$

with

$$C_{7\gamma}(M_W)^{\text{SM}} = -\frac{A(x_t)}{2}, \tag{18}$$

$$C_{8G}(M_W)^{\text{SM}} = -\frac{D(x_t)}{2}, \tag{19}$$

where $x_t = m_t^2/M_W^2$, $y_t = m_t^2/M_{H^+}^2$, the phase angle $\theta = \theta_b - \theta_t$, while θ_b (θ_t) is the phase angle of λ_{bb} (λ_{tt}). When compared with Eqs. (18),(19) of Ref. [33], the second and third terms in Eqs. (15) and (17) have an additional factor of $1/2$, since $\xi_{ij}^{U,D}$ used here has as additional factor $1/\sqrt{2}$. The Inami-Lim functions [34] (A, B, D, E) are of the form

$$A(x) = \frac{7x - 5x^2 - 8x^3}{12(1-x)^3} + \frac{2x^2 - 3x^3}{2(1-x)^4} \log[x], \qquad (20)$$

$$D(x) = \frac{2x + 5x^2 - x^3}{4(1-x)^3} + \frac{3x^2}{2(1-x)^4} \log[x], \qquad (21)$$

$$B(y) = \frac{-3y + 5y^2}{12(1-y)^2} - \frac{2y - 3y^2}{6(1-y)^3} \log[y], \qquad (22)$$

$$E(y) = \frac{-3y + y^2}{4(1-y)^2} - \frac{y}{2(1-y)^3} \log[y]. \qquad (23)$$

The Wilson coefficients given in Eqs. (12)–(17) contained the contributions from both the $W^{\pm}$-penguin and $H^{\pm}$-penguin diagrams.

It is easy to see that both $C_{7\gamma}^L(M_W)$ and $C_{8G}^L(M_W)$ in Eqs. (14) and (16) will be doubly suppressed by the ratio m_s/m_b and $|\lambda_{tt}|^2$ when $|\lambda_{tt}|$ is small as preferred by the data of neutron electric dipole moment (NEDM) [33]. For typical values of relevant parameters, say $|\lambda_{tt}| = 0.3$, $|\lambda_{bb}| = 40$, $\theta = 0^0$, and $M_{H^+} = 200$ GeV, One finds numerically that $C_{7\gamma}^L(M_W) \approx C_{8G}^L(M_W) \approx 10^{-5}$, while $C_{7\gamma}^R(M_W) \approx C_{8G}^R(M_W) \approx 0.8$. Consequently, the left-handed Wilson coefficients are much smaller than their right-handed counterparts and therefore will be neglected in the following calculations.

At the lower-energy scale $\mu = O(m_b)$, the Wilson coefficients $C_i(\mu)$ for the decay $b \to s\gamma$ at the leading order are of the form

$$C_j(\mu) = \sum_{i=1}^{6} k_{ji} \eta^{a_i} \quad (j = 1, \dots, 6), \qquad (24)$$

$$C_{7\gamma}(\mu)^{\mathrm{SM}} = \eta^{16/23} C_{7\gamma}(M_W)^{\mathrm{SM}}$$
$$+ \frac{8}{3}(\eta^{14/23} - \eta^{16/23}) C_{8G}(M_W)^{\mathrm{SM}} + \sum_{i=1}^{8} h_i \eta^{a_i},$$
$$\qquad (25)$$

$$C_{7\gamma}(\mu)^{\mathrm{III}} = \eta^{16/23} C_{7\gamma}^R(M_W) + \frac{8}{3}(\eta^{14/23} - \eta^{16/23}) C_{8G}^R(M_W)$$
$$+ \sum_{i=1}^{8} h_i \eta^{a_i}, \qquad (26)$$

where $\eta = \alpha_s(M_W)/\alpha_s(\mu)$, and the scheme-independent numbers a_i, k_{ji}, and h_i can be found in Ref. [4].

Using the effective Hamiltonian, the branching ratio of $b \to s\gamma$ at the leading order can be written as

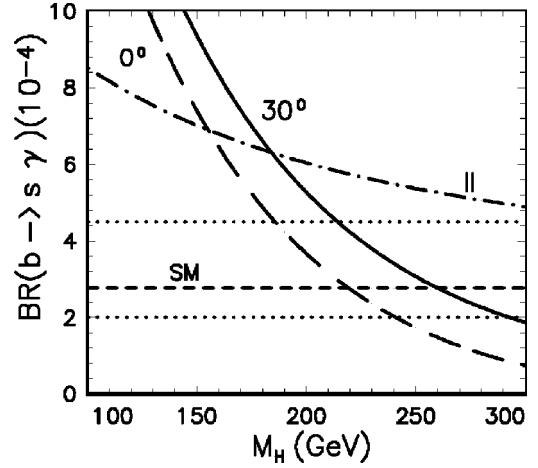FIG. 2. Plots of the branching ratio BR($b \to s\gamma$) versus M_{H^+} in the SM and models II and III. The short-dashed line is the SM prediction, and the band between two dots lines refers to the CLEO data. The dot-dashed curve shows the ratio in model II, while the long-dashed and solid curve show the ratios in model III for $\theta = 0°, 30°$, respectively.

$$\mathrm{BR}(b \to s\gamma)^{(\mathrm{III})} = \frac{|V_{ts}^* V_{tb}|^2}{|V_{cb}|^2} \frac{6\alpha_{em}}{\pi f(z)} |C_{7\gamma}(\mu)^{\mathrm{III}}|^2 \mathrm{BR}(b \to c e \bar{\nu}),$$
$$\qquad (27)$$

where $\mu = O(m_b)$, BR($b \to c e \bar{\nu}) = (10.7 \pm 0.4)\%$ is the measured semileptonic branching ratio of b decay, and $f(z)$ is the phase space factor

$$f(z) = 1 - 8z^2 + 8z^6 - z^8 - 24z^4 \log[z], \qquad (28)$$

where $z = m_c^{\mathrm{pole}}/m_b^{\mathrm{pole}}$. It is straightforward to write down the branching ratios BR($b \to s\gamma$) for the SM and model II.

In the numerical calculations, the following input parameters [15,35] will be used implicitly:

$$M_W = 80.41 \text{ GeV}, \quad M_Z = 91.187 \text{ GeV}, \quad \alpha_{em} = 1/137,$$

$$\alpha_s(M_Z) = 0.118, \quad G_F = 1.16639 \times 10^{-5} \text{ (GeV)}^{-2},$$

$$m_s = 0.13 \text{ GeV}, \quad m_c = 1.4 \text{ GeV}, \quad m_b = 4.8 \text{ GeV},$$

$$m_t = \overline{m}_t(m_t) = 168 \text{ GeV}, \quad \Lambda_{(5)}^{\overline{\mathrm{MS}}} = 0.225,$$

$$A = 0.84, \quad \lambda = 0.22, \quad \rho = 0.20, \quad \eta = 0.34, \qquad (29)$$

where A, λ, ρ, and η are the Wolfenstein parameters of the CKM mixing matrix. $\overline{m}_t(m_t)$ here refers to the running current top quark mass normalized at $\mu = m_t$ and is obtained from the pole mass $m_t^{\mathrm{pole}} = 176$ GeV. For the running of α_s, the two-loop formulas [4] will be used.

Figure 2 shows the branching ratios BR($b \to s\gamma$) in the SM and models II and III, assuming $\lambda_{tt} = 0.3$, $\lambda_{bb} = 35$, $\theta = 0°, 30°$, $\tan\beta = 1$. The horizontal band between two dotted lines corresponds to the CLEO data [9]: $2 \times 10^{-4} \leqslant \mathrm{BR}(b \to s\gamma) \leqslant 4.5 \times 10^{-4}$. The short-dashed line is the SM prediction, and the long-dashed and solid curve show the ratio in model III for $\theta = 0°, 30°$, respectively. The dot-dashed curve

shows the same ratio at the leading order in model II. From Fig. 2, the lower and upper limit on M_{H^+} in model III can be read out:

$$185 \text{ GeV} \leqslant M_{H^+} \leqslant 238 \text{ GeV}, \quad \text{for } \theta = 0°,$$

$$215 \text{ GeV} \leqslant M_{H^+} \leqslant 287 \text{ GeV}, \quad \text{for } \theta = 30°. \quad (30)$$

These limits are consistent with those given in Eq. (8). If we take into account the errors of theoretical predictions in model III, the corresponding mass limit will be relaxed by about 20 GeV.

From above analysis, we get to know that for model III the parameter space

$$\lambda_{ij} = 0, \quad \text{for } ij \neq tt, \quad \text{or} \quad bb,$$

$$|\lambda_{tt}| = 0.3, \quad |\lambda_{bb}| = 35, \quad \theta = (0° - 30°),$$

$$M_{H^+} = (200 \pm 100) \text{ GeV}, \quad (31)$$

are allowed by the available data. For the mass M_{H^+}, searches for pair production at LEP have excluded masses $M_{H^+} \leqslant 77$ GeV [36]. Combining the direct and indirect limits together, we here conservatively consider a larger range of 100 GeV $\leqslant M_{H^+} \leqslant 300$ GeV, while take $M_{H^+} = 200$ GeV as the typical value.

III. INCLUSIVE CHARMLESS b QUARK DECAYS

In this section, we will calculate the new physics contributions to the two-body and three-body inclusive charmless decays of b quark induced by the charged Higgs gluonic penguin diagrams in models II and III.

A. $b \rightarrow s$ gluon decay

The branching ratio of $b \rightarrow sg$ at the leading order can be written as

$$\text{BR}(b \rightarrow sg) = \frac{|V_{ts}^* V_{tb}|^2}{|V_{cb}|^2} \frac{8\alpha_s(\mu)}{\pi f(z)\kappa(z)} |C_{8G}(\mu)|^2 \text{BR}(b \rightarrow ce\bar{\nu}),$$
$$(32)$$

with

$$C_{8G}(\mu)^{\text{SM}} = \eta^{14/23} C_{8G}(M_W)^{\text{SM}} + \sum_{i=1}^{8} \bar{h}_i \eta^{a_i}, \quad (33)$$

$$C_{8G}(\mu)^{\text{III}} = \eta^{14/23} C_{8G}^R(M_W) + \sum_{i=1}^{8} \bar{h}_i \eta^{a_i}, \quad (34)$$

where $\eta = \alpha_s(M_W)/\alpha_s(\mu)$ with $\mu = O(m_b)$, and the numbers a_i and $\bar{h}_i$ can be found in Ref. [4]. The factor $\kappa(z)$ contains the QCD correction to the semileptonic decay rate $\text{BR}(b \rightarrow ce\bar{\nu})$ [37–39]. To a good approximation the $\kappa(z)$ is given by [39]

$$\kappa(z) = 1 - \frac{2\alpha_s(\mu)}{3\pi} \left[\left(\pi^2 - \frac{31}{4} \right)(1-z)^2 + \frac{3}{2} \right] \quad (35)$$
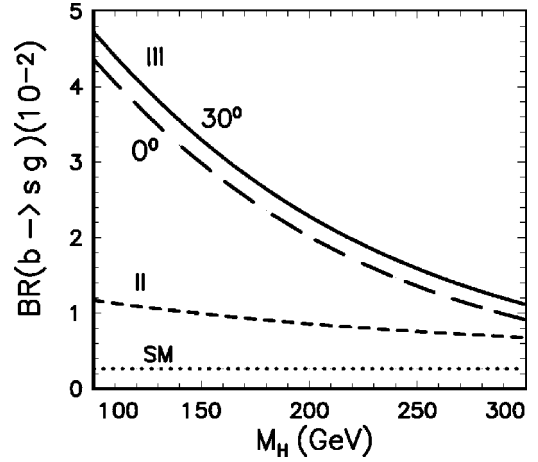

FIG. 3. Plots of the branching ratio $\text{BR}(b \rightarrow sg)$ versus M_{H^+} in the SM and models II and III. The dots line is the SM prediction, the short-dashed curve shows the the ratio in model II, and the long-dashed and solid curve show the ratios in model III for $\theta = 0°, 30°$, respectively.

and an exact analytic formula for $\kappa(z)$ can be found in Ref. [38].

For $b \rightarrow dg$ decay, one simply substitutes V_{ts}^* by V_{td}^* in Eq. (32). For model II, one simply replaces $C_{8G}(\mu)$ in Eq. (32) with C_{8G}^{II} as given in Ref. [27].

Figure 3 shows the branching ratios of $\text{BR}(b \rightarrow sg)$ in the SM and models II and III, assuming $\lambda_{tt} = 0.3$, $\lambda_{bb} = 35$, and $\theta = 0^0$, 30^0. The dots line in Fig. 3 is the SM prediction $\text{BR}(b \rightarrow sg) = 0.27\%$, while the short-dashed curve shows the branching ratio $\text{BR}(b \rightarrow sg) = 0.81\%$ in model II assuming $\tan \beta = 2$ and $M_{H^+} = 200$ GeV. In model III, the enhancement to the ratio $\text{BR}(b \rightarrow sg)$ can be as large as an order of magnitude: $\text{BR}(b \rightarrow sg) \approx 2.34\%$, 4.84% for $M_{H^+} = 200$, 100 GeV respectively, as illustrated by the long-dashed and solid curves in Fig. 3. Model III is clearly more promising than model II to provide a large enhancement to the decay $b \rightarrow sg$. Although the current enhancement is still smaller than $\sim 10\%$ as expected, for example in Refs. [19,23], such a significant increase is obviously very helpful for us to provide a reasonable solution for the problems such as the ''missing charm puzzle'' or the deficit B_{SL}, as being discussed below.

B. Three-body charmless b quark decays

Within the SM, the three-body inclusive charmless b quark decays have been calculated at LO and NLO level for example in Refs. [6,24,40]. In Ref. [6], Lenz et al. took into account the NLO QCD corrections from the gluonic penguin diagrams with insertions of Q_2 and the diagrams involving the interference of the Q_{8G} with Q_{1-6} [6].

The standard theoretical frame to calculate the decays $b \rightarrow sq\bar{q}$ for $q \in \{u,d,s\}$ is based on the effective Hamiltonian [1]

$$\mathcal{H}_{\text{eff}}(|\Delta B|=1)=\frac{G_F}{\sqrt{2}}\left\{\sum_{j=1}^{2}C_j(v_cQ_j^c+v_uQ_j^u)\right.$$
$$\left.-v_t\left[\sum_{j=3}^{6}C_jQ_j+C_8Q_{8G}\right]\right\}+\text{H.c.,}$$

(36)

where $v_q=V_{qs}^*V_{qb}$ and the corresponding operator basis reads

$$Q_1=(\bar{s}_\alpha q_\beta)_{V-A}(\bar{q}_\beta b_\alpha)_{V-A},$$ (37)

$$Q_2=(\bar{s}_\alpha q_\alpha)_{V-A}(\bar{q}_\beta b_\beta)_{V-A},$$ (38)

with $q=u$ and $q=c$, and

$$Q_3=(\bar{s}_\alpha b_\alpha)_{V-A}\sum_{q=u,d,s}(\bar{q}_\beta q_\beta)_{V-A},$$ (39)

$$Q_4=(\bar{s}_\alpha b_\beta)_{V-A}\sum_{q=u,d,s}(\bar{q}_\beta q_\alpha)_{V-A},$$ (40)

$$Q_5=(\bar{s}_\alpha b_\alpha)_{V-A}\sum_{q=u,d,s}(\bar{q}_\beta q_\beta)_{V+A},$$ (41)

$$Q_6=(\bar{s}_\alpha b_\beta)_{V-A}\sum_{q=u,d,s}(\bar{q}_\beta q_\alpha)_{V+A},$$ (42)

$$Q_{8G}=-\frac{g_s}{8\pi^2}m_b\bar{s}_\alpha\sigma^{\mu\nu}(1+\gamma_5)T_{\alpha\beta}^a b_\beta G_{\mu\nu}^a,$$ (43)

where the Q_1 and Q_2 are current-current operators, Q_3-Q_6 are QCD penguin operators, while the Q_{8G} is the chromomagnetic dipole operator.

For the SM part, we will use the formulas presented in Ref. [6] directly. For the new physics part in models II and III under study here, we take into account the new contributions from charged-Higgs gluonic penguin diagrams by using the Wilson coefficient $C_{8G}(\mu)^{\text{III}}$ as given in Eq. (34) in the calculation, this coefficient comprises both the SM and the new physics contributions. All other Wilson coefficients remain unmodified.

When the NLO QCD corrections are included, one usually expand the decay width to order α_s,

$$\Gamma(b\to sq\bar{q})=\Gamma^{(0)}+\frac{\alpha_s(\mu)}{4\pi}(\Delta\bar{\Gamma}_{cc}+\Delta\bar{\Gamma}_{\text{peng}}$$
$$+\Delta\bar{\Gamma}_W+\Delta\Gamma_8)+O(\alpha_s^2),$$ (44)

where $\Gamma^{(0)}$ denotes the decay rate at the LO level, while the second part represents the NLO QCD corrections. We here use the renormalization-scheme (RS) independent terms $\Delta\bar{\Gamma}_{cc}$, $\Delta\bar{\Gamma}_{\text{peng}}$, and $\Delta\bar{\Gamma}_W$. For the convenience of the reader, the explicit expressions of $\Delta\bar{\Gamma}_{cc}$, $\Delta\bar{\Gamma}_{\text{peng}}$, and $\Delta\bar{\Gamma}_W$ will be given in the Appendix. The term $\Delta\Gamma_8$ in Eq. (44) [which will be defined below in Eq. (52)] is already RS independent

[6,35]. For the three-body decays $b\to dq\bar{q}$ one simply substitutes s by d in Eqs. (36)–(44).

At the NLO, the RS dependent Wilson coefficients $C_j(\mu)$ are given by [35]

$$C_j(\mu)=C_j^{(0)}(\mu)+\frac{\alpha_s(\mu)}{4\pi}C_j(\mu)^{(1)},\quad j=1,\ldots,6,$$

(45)

where $C_j^{(0)}$ are the RS independent LO Wilson coefficients, and $C_j^{(1)}$ are the RS dependent NLO corrections [35]

$$C_j^{(0)}(\mu_b)=\sum_{i=3}^{8}k_{ji}\eta^{a_i},$$ (46)

$$C_j^{(1)}(\mu_b)=\sum_{i=3}^{8}[e_{ji}\eta E_0(x_t)+f_{ji}+g_{ji}\eta]\eta^{a_i},$$ (47)

where $\eta=\alpha_s(M_W)/\alpha_s(\mu_b)$, $x_t=m_t^2/M_W^2$, the function $E_0(x_t)$ and all the numbers a_i, k_{ji}, e_{ji}, f_{ji}, and g_{ji} can be found in Ref. [35]. The NLO QCD correction $C_j^{(1)}$ is RS dependent and can be split into two parts:

$$C_j(\mu)^{(1)}=\sum_{k=1}^{6}J_{jk}C_k^{(0)}(\mu)+\bar{C}_j(\mu)^{(1)},\quad j=1,\ldots,6,$$

(48)

where parameters J_{jk} are usually RS dependent, $\bar{C}_j(\mu)^{(1)}$ is RS independent, and the precise definitions of the terms in Eq. (48) can be found, for example, in Ref. [41]. The terms involving J_{jk} will be absorbed into $\Delta\bar{\Gamma}_{cc}$ and $\Delta\bar{\Gamma}_{\text{peng}}$ to make the latter scheme independent.

In the leading order the decays $b\to ss\bar{s}$, $sd\bar{d}$, $ds\bar{s}$, and $dd\bar{d}$ are penguin-induced processes proceeding via Q_{3-6} and Q_{8G}, while $b\to du\bar{u}$ and $b\to su\bar{u}$ also receive contributions from Q_1 and Q_2. Combining both cases, the decay width at the LO level can be written as [6]

$$\Gamma^{(0)}=\frac{G_F^2m_b^5}{64\pi^3}\left\{t\sum_{i,j=1}^{2}|v_u|^2C_i^{(0)}C_j^{(0)}b_{ij}\right.$$
$$+\sum_{i,j=3}^{6}|v_t|^2C_i^{(0)}C_j^{(0)}b_{ij}$$
$$\left.-2t\sum_{\substack{i=1,2\\j=3,\ldots6}}C_i^{(0)}C_j^{(0)}\text{Re}(v_uv_t^*)b_{ij}\right\}$$ (49)

with $t=1$ for $q=u$ and $t=0$ for $q=d,s$. The coefficients b_{ij} read

$$b_{ij}=\frac{16\pi^3}{m_b^6}\int d\Phi_3(2\pi)^4\overline{\langle Q_i\rangle^{(0)}\langle Q_j\rangle^{(0)*}}=b_{ji}$$ (50)

with $Q_{1,2}=Q_{1,2}^u$ here. Setting the final state quark masses to zero one finds [6]

$$b_{ij} = \begin{cases} 1 + r/3 & \text{for } i, j \leqslant 4, \text{ and } i + j \text{ even}, \\ 1/3 + r & \text{for } i, j \leqslant 4, \text{ and } i + j \text{ odd}, \end{cases}$$

$$b_{55} = b_{66} = 1, \quad b_{56} = b_{65} = 1/3. \tag{51}$$

Here $r = 1$ for the decays $b \to d d \bar{d}$ and $b \to s s \bar{s}$, in which the final state contains two identical particles, and $r = 0$ otherwise. The remaining b_{ij}'s are zero.

Now we turn to study the contributions from the interference of the tree diagram with Q_8 with operators Q_{1-6}, as shown in Fig. 3 of Ref. [6]. The tree-level correction $\Delta\Gamma_8$ is already at the order of α_s and is given by

$$\Delta\Gamma_8 = \frac{G_F^2 m_b^5}{32\pi^3} \mathrm{Re}\left[-t \, v_u^* v_t C_{8G}(\mu)^{\mathrm{III}} \sum_{j=1}^{2} C_j^{(0)} b_{j8} \right.$$

$$\left. + |v_t|^2 C_{8G}(\mu)^{\mathrm{III}} \sum_{j=3}^{6} C_j^{(0)} b_{j8} \right] \tag{52}$$

in model III, where $C_{8G}(\mu)^{\mathrm{III}}$ has been given in Eq. (34) with $\mu = O(m_b)$. For the case of the SM and model II, simply replace $C_{8G}(\mu_b)^{\mathrm{III}}$ with the appropriate $C_{8G}(\mu_b)$. The definitions and numerical values of coefficients b_{j8} can be found in Ref. [6]. As mentioned previously, the Wilson coefficient C_{8G}^{III} now comprises the contributions from both the W-penguin and the charged-Higgs penguin diagrams. In this way, the new physics contributions are taken into account.

For the b quark decay rates one usually normalize them to the semileptonic decay rate of the b quark

$$r_{ql} = \frac{\Gamma(b \to q l \bar{\nu}_l)}{\Gamma(b \to c e \bar{\nu}_e)}, \quad r_{qg} = \frac{\Gamma(b \to q g)}{\Gamma(b \to c e \bar{\nu}_e)},$$

$$r_{q_1 q_2 \bar{q}_3} = \frac{\Gamma(b \to q_1 q_2 \bar{q}_3)}{\Gamma(b \to c e \bar{\nu}_e)}, \quad r_{sgg} = \frac{\Gamma(b \to s g g)}{\Gamma(b \to c e \bar{\nu}_e)}, \tag{53}$$

for the sake of eliminating the factor of m_b^5 common to all b decay rates. One also define the charmless decay rate of b quark as

$$r_{\ell} = \sum_{q = u, d, s} (r_{dq\bar{q}} + r_{sq\bar{q}}) + r_{sg} + r_{dg} + r_{sgg} + 2r_{ue} + r_{u\tau}, \tag{54}$$

where rare radiative decays, for example $b \to s \gamma$, have been neglected. To order α_s, the semileptonic decay rate takes the form

$$\Gamma(b \to c e \bar{\nu}_e) = \frac{G_F^2 m_b^5}{192\pi^3} |V_{cb}|^2 f(z) \kappa(z), \tag{55}$$

where the factors $f(z)$ and $\kappa(z)$ have been given in Eqs. (28) and (35).

To calculate r_{ℓ} we also need explicit expressions of r_{ue}, r_{sg}, r_{dg} and r_{sgg}. For r_{ue} one finds [42]

$$r_{ue} = \frac{|V_{ub}|^2}{|V_{cb}|^2} \frac{1}{f(z)} \left\{ 1 + \kappa(z) - \kappa(0) + 6\left[\frac{(1 - z^2)^4}{f(z)} - 1 \right] \frac{\lambda_2}{m_b^2} \right\}, \tag{56}$$

where $\lambda_2 = 0.12 \text{ GeV}^2$ encodes the chromomagnetic interaction of the b quark with light degrees of freedom, and the factors of $f(z)$ and $\kappa(z)$ have been given in Eqs. (28) and (35).

From Eq. (32), we get

$$r_{sg} = \frac{|V_{ts}^* V_{tb}|^2}{|V_{cb}|^2} \frac{8\alpha_s(\mu)}{\pi f(z) \kappa(z)} |C_{8G}(\mu)|^2, \tag{57}$$

$$r_{dg} = \frac{|V_{td}^* V_{tb}|^2}{|V_{cb}|^2} \frac{8\alpha_s(\mu)}{\pi f(z) \kappa(z)} |C_{8G}(\mu)|^2. \tag{58}$$

For r_{sgg}, we use the formulas as given in Refs. [40,24],

$$r_{sgg} = \frac{1}{|V_{cb}|^2} \frac{3\alpha_s(\mu)^2}{16\pi^2 f(z) \kappa(z)} \left| \sum_{i = u, c, t} V_{is}^* V_{ib} f_1(x_i, q^2) \right|^2, \tag{59}$$

where $x_i = m_i^2/M_W^2$, the functions $f_1(x_i, q^2)$ can be found, for example, in Ref. [24]. In the numerical calculation, we assume that $q^2 = m_b^2/2$. Since the new contribution to the decay $b \to s g g$ due to the charged Higgs penguin diagram is negligibly small [24], we do not consider the new physics corrections to this decay here. In Ref. [6], the authors did not include r_{sgg} in the estimation of r_{ℓ}. We here will include this mode, since its branching ratio is rather large [40,24], as shown in Table I.

The corresponding branching ratios for two-body and three-body charmless b decays are defined as

$$\mathrm{BR}(b \to X) = r_X \, \mathrm{BR}(b \to c e \bar{\nu}_e)^{\mathrm{exp}}, \tag{60}$$

where ratios r_X have been defined previously. In the numerical calculations, $\mathrm{BR}(b \to c \bar{\nu}_e)^{\mathrm{exp}} = 10.70\%$ will be used.[2]

By using the input parameters as given in Eq. (29) and assuming $|\lambda_{tt}| = 0.3$, $|\lambda_{bb}| = 35$, $M_{H^+} = 200$ GeV and $\theta = 0°$ or $30°$, we find the numerical results of the decay rates and the branching ratios for various charmless b quark decays and collect them in Table I. We also show the corresponding results in model II assuming $M_{H^+} = 200$ GeV and $\tan\beta = 2$. For larger $\tan\beta$ the new physics contributions in model II will become smaller. $\Delta\mathrm{BR}$ in Table I is defined as

$$\Delta\mathrm{BR}(b \to X) = [\mathrm{BR}(b \to X)$$
$$- \mathrm{BR}(b \to X)^{\mathrm{SM}}]/\mathrm{BR}(b \to \mathrm{SM})^{\mathrm{SM}}. \tag{61}$$

Figure 4 shows the mass dependence of the branching ratios $\mathrm{BR}(b \to s q \bar{q})$ with $q \in \{u, d, s\}$ in the SM and model III, using the input parameters in Eq. (29) and assuming $|\lambda_{tt}| = 0.3$, $|\lambda_{bb}| = 35$, and $\theta = 30°$. In Fig. 4, the three curves

---

[2]For more details, one can see the discussions about the semileptonic branching ratios of b decay in next section.

TABLE I. The rates r and branching ratios in the SM and models II and III, assuming $|\lambda_{tt}|=0.3$, $|\lambda_{bb}|=35$, $M_{H^+}=200$ GeV, $\tan\beta=2$, and $\theta=0°$ or $30°$ (the numbers in parenthesis). We also use BR($B\rightarrow X_c e\bar{\nu}_e)^{\exp}=10.70\%$ as given in Eq. (63).

| decay mode | SM | | Model III | | | Model II |
	r	BR(%)	r	BR (%)	ΔBR(%)	ΔBR(%)
$b\rightarrow d\,u\bar{u}$	0.051	0.545	0.052	0.554	1.6	-0.3
			(0.053)	(0.571)	(4.7)	
$b\rightarrow d\,d\bar{d}$	0.0005	0.006	0.00078	0.103	68.2	-13.4
			(0.0007)	(0.010)	(59.0)	
$b\rightarrow d\,s\bar{s}$	0.0006	0.005	0.00096	0.008	68.7	-13.5
			(0.0009)	(0.008)	(59.5)	
$b\rightarrow s\,u\bar{u}$	0.018	0.192	0.027	0.286	49.0	-9.6
			(0.0237)	(0.255)	(32.8)	
$b\rightarrow s\,d\bar{d}$	0.019	0.206	0.030	0.322	56.0	-11.0
			(0.0285)	(0.307)	(48.5)	
$b\rightarrow s\,s\bar{s}$	0.016	0.168	0.024	0.262	56.7	-9.9
			(0.0232)	(0.250)	(49.2)	
$b\rightarrow s\,g$	0.025	0.270	0.192	2.065	663.6	202.3
			(0.217)	(2.339)	(765.0)	
$b\rightarrow d\,g$	0.00092	0.010	0.007	0.070	663.6	202.3
			(0.008)	(0.086)	(765.0)	
$b\rightarrow s\,gg$	0.070	0.757	0.070	0.757		
$b\rightarrow u\,e\bar{\nu}_e$	0.013	0.144	0.013	0.144		
$b\rightarrow u\,\mu\bar{\nu}_\mu$	0.013	0.144	0.013	0.144		
$b\rightarrow u\,\tau\bar{\nu}_\tau$	0.004	0.0004	0.004	0.0004		
$b\rightarrow no\ charm$	0.23	2.49	0.43	4.67	87.6	20.3
			(0.46)	(4.91)	(97.3)	

(horizontal lines) are the theoretical predictions in model III (SM) for $q=u,d,s$, respectively. For $M_{H^+}=200$ GeV, as listed in Table I, the enhancement to the decay mode $b\rightarrow d\,u\bar{u}$ is only 4.7%, but the enhancements to other five three-body b quark decay modes are rather large: from $\sim$30 to $\sim$70%. In model II, however, the new contributions are negative and will decrease the branching ratios slightly, from -0.3 to -13.5% for different decay modes.

Figure 5 shows the branching ratio BR($b\rightarrow$no charm) in the SM and models II and III, using the input parameters in Eq. (29) and assuming $|\lambda_{tt}|=0.3$, $|\lambda_{bb}|=35$, and $\theta=0°$, $30°$. The dotted line in Fig. 5 is the SM prediction BR($b\rightarrow$no charm)$=2.49\%$. The short-dashed curve shows the the ratio in the model II, BR($b\rightarrow$no charm)$=2.98\%$ (3.23%) for $M_{H^+}=200$ (100) GeV and $\tan\beta=2$. The long-dashed and solid curve show the theoretical predictions in the model III: BR($b\rightarrow$no charm)$=4.67\%$ (4.91%) for $M_{H^+}=200$ GeV and $\theta=0°,30°$, respectively. For the model III with $M_{H^+}=100$ GeV, one finds that BR($b\rightarrow$no charm)$=7.27\%$ (7.60%) for $\theta=0°,30°$, respectively. It is easy to see from Fig. 5 and Table I that the new physics enhancement to the branching ratios of three-body charmless b quark decays in the model III is much larger than that in model II within the parameter space considered.
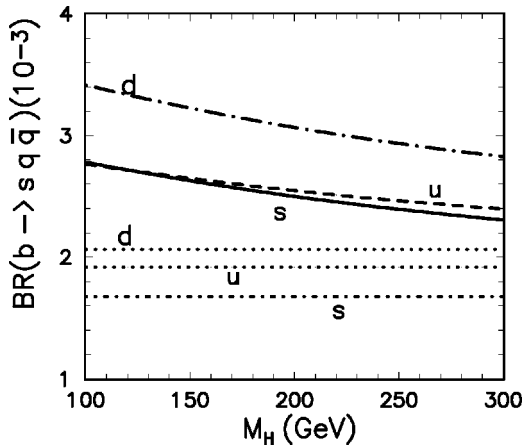

FIG. 4. Plots of branching ratio BR($b\rightarrow sq\bar{q}$) versus M_{H^+} in model III. The three curves (horizontal lines) are the theoretical predictions in model III (SM) for $q=u,d,s$, respectively.

IV. n_c AND $B_{\rm SL}$

The ratio $B_{\rm SL}$ is the average over weakly decaying hadrons containing one b quark. For the CLEO experiments running on the $\Upsilon(4S)$ resonance, the average is over B^+ and B° and their charge conjugate hadrons. For the experiments run-
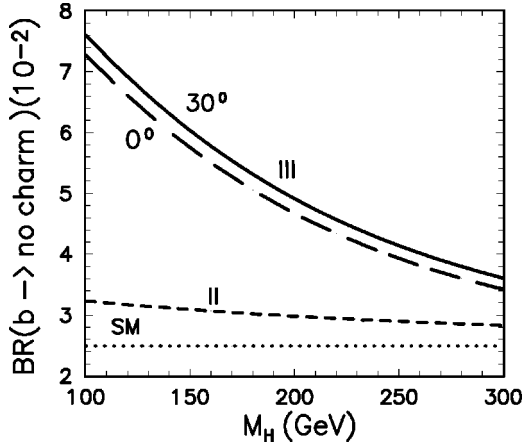
FIG. 5. Plots of the branching ratios $BR(b\rightarrow \text{no charm})$ versus M_{H^+} in the SM and models II and III. The dots line is the SM prediction, the short-dashed curve shows the ratio in model II, and the long-dashed and solid curve show the theoretical predictions in the model III for $\theta=0°,30°$, respectively.

ning on $Z°$ resonance, however, the average is over B^+, $B°$, $B_s^°$, and N_b.[3]

The charm multiplicity n_c is the average over the b hadrons produced in the given environment. CLEO and LEP Collaborations presented new measurements of inclusive $b\rightarrow c$ transitions that can be used to extract n_c. One naively expect $n_c=1.15$ with the additional 15% coming from the tree-level decay chain $b\rightarrow uW^-\rightarrow u\bar{c}s$. This expectation can be verified experimentally by adding all inclusive $b\rightarrow c$ branching ratios, and counting twice for the decay modes with two charm quarks in the final state. In this section, we will investigate the new physics contributions, induced by the charged Higgs penguins in models II and III, to the ratio B_{SL} and the charm multiplicity n_c.

A. n_c and B_{SL}: Experimental measurements

The B_{SL} deficit was first pointed out around 1994 [13] when the theoretical prediction was considered to be difficult to produce $B_{SL}\lesssim 12\%$ while the 1995 CLEO data on $\Upsilon(4S)$ resonance was $B_{SL}=(10.49\pm0.46)\%$ [14]. In the following, we use the 1998 Particle Data Group value [15]

$$B_{SL}=(10.45\pm0.21)\% \qquad (62)$$

as the measured B_{SL} on $\Upsilon(4S)$.

For the experiments on the $Z°$ peak, all the four LEP collaborations [43–46] reported their measured values of the ratio B_{SL} as listed in Table II. The seventh row shows the averaged result of the ratio B_{SL} on the $Z°$ peak:[4] $B_{SL}^b=(10.66\pm0.17)\%$. This B_{SL}^b on the $Z°$ peak can be con-

---

[3]N_b is in turn the mixture of $\Lambda_b(udb)$, $\Sigma_b(usb)$, $\Xi_b(dsb)$, and $\Omega_b(ssb)$.

[4]We here made an arithmetic average over four results as done in Ref. [18], but the newest L3 data [45] has been used here in the average.

TABLE II. Recent CLEO and LEP measurements of the ratio B_{SL}.

$B_{SL}(\%)$	Experiment
10.45 ± 0.21	$\Upsilon(4S)$ PDG98 [15]
$11.01\pm0.10(\text{stat})\pm0.30(\text{syst})$	ALEPH 95 [43]
$10.65\pm0.07(\text{stat})\pm0.25(\text{syst})^{+0.28}_{-0.12}(\text{model})$	DELPHI 99 [44]
$10.16\pm0.13(\text{stat})\pm0.30(\text{syst})$	L3 99 [45]
$10.83\pm0.10(\text{stat})\pm0.20(\text{syst})^{+0.20}_{-0.13}(\text{model})$	OPAL 99 [46]
10.66 ± 0.17	$Z°$-peak
10.94 ± 0.19	$Z°$ corrected
10.70 ± 0.21	overall average

verted to $\Upsilon(4S)$ value by multiplying a factor of $\tau_B/\tau_b=1.026$: $B_{SL}=(10.94\pm0.19)\%$ ($Z°$ corrected). In fact, there is still a 2σ discrepancy in ratio B_{SL} between the high-energy $Z°$ value and the low-energy $\Upsilon(4S)$ value. The average of the $Z°$ and $\Upsilon(4S)$ values of B_{SL} is

$$B_{SL}=(10.70\pm0.21)\%, \quad \text{Overall average,} \qquad (63)$$

where we conservatively chose 0.21 as the overall error of the measured B_{SL}.

As for the charm counting, the value of n_c measured at the $\Upsilon(4S)$ [20] is still smaller than that measured at the $Z°$ peak [15]:

$$n_c=\begin{cases} 1.10\pm0.05, & \Upsilon(4S), \\ 1.20\pm0.07, & Z°\text{peak}. \end{cases} \qquad (64)$$

The average of the $\Upsilon(4S)$ and $Z°$ result leads to

$$n_c=1.14\pm0.04 \ [Z°+\Upsilon(4S)] \qquad (65)$$

B. n_c and B_{SL}: Theoretical predictions

Within the SM, the basis of the prediction for B_{SL} and n_c is the assumption of quark-hadron duality. The estimation for various inclusive decay rates is usually performed by using the heavy-quark expansion (HQE) [47] and the perturbative QCD in the framework of the operator product expansion. The HQE allows us to relate the inclusive decay rate of the B meson to that of the underlying b quark decay process $\Gamma(B\rightarrow X)=\Gamma(b\rightarrow x)+O(1/m_b^2)$.

The theoretical prediction for B_{SL} with the inclusion of the $O(\alpha_s)$ QCD corrections and the hadronic corrections to the free quark decay of order $1/m_b^2$ is currently available [16,17]. B_{SL} and n_c can be defined as [16,17]

$$B_{SL}=\frac{1}{\sum_l r_{cl}+r_{c\bar{u}d}+r_{c\bar{c}s}+r_\ell}, \qquad (66)$$

$$n_c=1+\frac{r_{c\bar{c}s}-r_\ell}{\sum_l r_{cl}+r_{c\bar{u}d}+r_{c\bar{c}s}+r_\ell}, \qquad (67)$$

where $r_{ce} = r_{c\mu} = 1$, $r_{c\tau} = 0.25$, and $r_{c\bar{u}d}$ ($r_{c\bar{c}s}$) is the rate of the decay mode $b \to c\bar{u}d'$ ($b \to c\bar{c}s'$) where d' (s') is the appropriate Cabibbo mixture of d and s quarks.

The r_ℓ has been defined and calculated in the last section. In the SM, we have

$$r_\ell = 0.23 \pm 0.08, \tag{68}$$

where the error mainly comes from the uncertainties of the scale μ and the mass ratio m_c/m_b [6].

As is well known, the main difficulty in calculating B_{SL} and n_c is in the nonleptonic branching ratios $r_{c\bar{u}d}$ and $r_{c\bar{c}s}$. For $r_{c\bar{u}d}$, a complete NLO calculation has been performed [16] which gives

$$r_{c\bar{u}d} = 4.0 \pm 0.4, \tag{69}$$

where the error mainly comes from the uncertainties of the scale μ, the quark masses m_c and m_b, and the assumption of quark-hadron duality [16]. Furthermore, the error of the estimation for $r_{c\bar{c}s}$ is generally considered to be larger than that for $r_{c\bar{u}d}$. The enhancement of $b \to c\bar{c}s$ due to large QCD corrections is about 30% [16]. Such enhancement will decrease the value of B_{SL}, but increase the size of n_c.

Using the on-mass-shell sheme, the SM theoretical predictions for B_{SL} and n_c at the NLO level are

$$B_{SL} = (12.0 \pm 0.7 \pm 0.5 \pm 0.2^{+0.9}_{-1.2})\%, \tag{70}$$

$$n_c = 1.24 \mp 0.05 \pm 0.01, \tag{71}$$

as given[5] in Ref. [16] and

$$B_{SL} = \begin{cases} (12.0 \pm 1.0)\% & \mu = m_b, \\ (10.9 \pm 1.0)\% & \mu = m_b/2, \end{cases} \tag{72}$$

$$n_c = \begin{cases} 1.20 \mp 0.06 & \mu = m_b, \\ 1.21 \mp 0.06 & \mu = m_b/2, \end{cases} \tag{73}$$

as given in Ref. [17] with the error mainly result from the variation of the scale μ and m_c/m_b.

Comparing the observed and predicted values of B_{SL} and n_c, one can see that (a) after considering all the corrections, the theoretical values of B_{SL} now come down and more or less consistent with the measurement, but unfortunately at the expense of boosting n_c, (b) the central value of n_c in Ref. [16] is higher than that in Ref. [17], although two predictions are agree within errors, and (c) there is still 2.8σ discrepancy between the n_c measured by CLEO and the theoretical prediction [16]: 1.10 ± 0.05 against 1.24 ± 0.05.

If we drop down the large uncertainty in the calculation for $b \to c\bar{c}s'$ decay mode, we can eliminate the ratio $r_{c\bar{c}s'}$ from the expression of B_{SL} and n_c and find

$$n_c = 2 - (2.25 + r_{c\bar{u}d} + 2r_\ell)B_{SL} \tag{74}$$

---

[5]The last and largest error of B_{SL} comes from the uncertainty of the renormalization scale μ, while the main error of n_c is the the uncertainty in m_b [16].

which is a linear correlation between B_{SL} and n_c. Using the values for B_{SL} (63), $r_{c\bar{u}d}$ (69), and r_ℓ (68), one finds

$$n_c = 1.28 \pm 0.05, \tag{75}$$

for $B_{SL} = (10.70 \pm 0.21)\%$. The overall uncertainty of this prediction of n_c should be smaller than that as given in Eqs. (71) and (73). The 2.6σ discrepancy between the n_c in Eq. (75) and n_c measured at $\Upsilon(4S)$ motivated proposals of new physics which will enhance r_ℓ and in turn decrease n_c. That is what we try to do here.

As shown in Table I, the ratio r_ℓ will be increased significantly after taking the new physics effects into account, which will in turn decrease both B_{SL} and n_c accordingly. From Eq. (74) and using the values for B_{SL} (63), $r_{c\bar{u}d}$ (69), and r_ℓ (54), one finds

$$n_c = \begin{cases} 1.23 \pm 0.05 & \text{for } M_{H^+} = 200 \text{ GeV}, \\ 1.18 \pm 0.05 & \text{for } M_{H^+} = 100 \text{ GeV} \end{cases} \tag{76}$$

for $\theta = 30°$ and $\mu = m_b$. The μ and θ dependence of n_c is rather weak: the central value of n_c will go down (up) by only ~ 0.01 for $\mu = m_b/2$ ($\theta = 0°$). For B_{SL} in model III, the agreement between the prediction and the data will be improved slightly by a decrease 0.003 (0.005) for $M_{H^+} = 200$ (100) GeV due to the inclusion of new physics contributions. In model II, the resulted decrease for n_c (B_{SL}) is only 0.01 (0.001) and plays no real role. Most importantly, one can see from Eqs. (64), (65), (75), (76) that the predicted n_c and the measured n_c now agree within roughly one standard deviation after taking into account the effects of gluonic charged Higgs penguin diagrams in model III with a relatively light charged Higgs boson, as illustrated in Fig. 6.

V. SUMMARY AND DISCUSSIONS

In the framework of the general two-Higgs doublet models, we calculated the charged-Higgs penguin contributions to (a) the rare radiative decay $b \to s\gamma$, (b) the inclusive charmless decays $b \to q'g$ and $b \to q'q\bar{q}$ with $q' \in \{d,s\}$ and $q \in \{u,d,s\}$, and (c) the charm multiplicity n_c and semileptonic branching ratio B_{SL}.

In Sec. II, we studied the experimental constraint on model III from the CLEO data of $b \to s\gamma$ decay. With the help of previous works [26,31–33], we found the parameter space of the model III allowed by the available data, as shown in Eq. (31).

In Sec. III, we first calculated the new physics contributions to the decay $b \to sg$ and found that the branching ratio BR$(b \to sg)$ can be greatly enhanced from the SM prediction of 0.27 to 2.34 % (4.84%) in model III for $M_{H^+} = 200$ (100) GeV, as illustrated in Fig. 3. Such a significant enhancement is clearly very helpful to resolve the missing charm-B_{SL} problem appeared in B experiments.

Following the method of Ref. [6], we then calculated the new physics contributions to three-body inclusive charmless decays of b quark due to the interference between the operators Q_{1-6} and Q_{8G}. The Wilson coefficient C_{8G}^{III} in Eq. (34) now describe the contributions from both the $W^\pm$ and $H^\pm$ QCD penguins, the latter is the new physics part we focus on here. From numerical calculations we found that (a) the new
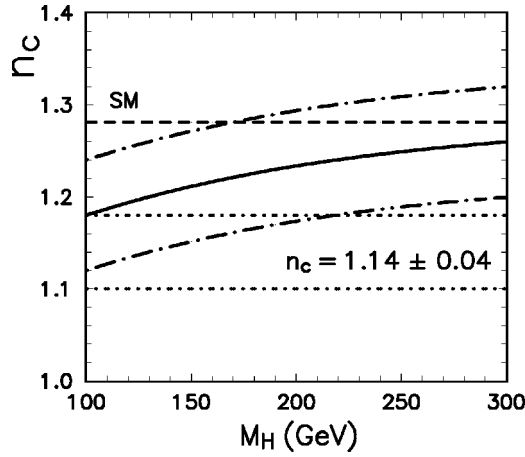
FIG. 6. Plots of Charm multiplicity n_c versus M_{H^+} in the SM and model III for $B_{SL} = 10.70\%$. The short-dashed line is the SM prediction, and the band refers to the data of $n_c = 1.14 \pm 0.04$. The solid curve, the upper and lower dot-dashed curves together show the central value and the 1σ error of the theoretical prediction for n_c in model III.

physics enhancement to the decay $b \to du\bar{u}$ is only $\sim 1.6\%$ since this mode is dominated by the tree diagrams, (b) the branching ratios of other five three-body b decay modes are strongly enhanced by the new charged Higgs penguins: 30 to 70 % increase can be achieved within the considered parameter space. The new contributions to the corresponding branching ratios in model II is, however, small in size and negative in sign against the theoretical predictions in the SM. As shown in Table I and Fig. 5, the ratio BR($b \to$no charm) can be increased from the SM prediction BR($b \to$no charm)$= 2.49\%$ to BR($b \to$no charm)$= 4.91\%$ (7.60%) in model III for $M_{H^+} = 200$ (100) GeV.

In Sec. IV, we examined the current status about the theoretical predictions and experimental measurements for the semileptonic branching ratio of B meson decay B_{SL} and the charm multiplicity n_c, and calculated the new physics contributions, induced by the charged Higgs penguin diagrams in model III (II), to both B_{SL} and n_c. With an enhanced ratio BR($b \to$no charm), both the B_{SL} and n_c will be decreased accordingly: (a) the central value of B_{SL} can be decreased slightly by 0.003 (0.005) for $M_{H^+} = 200$ (100) GeV, (b) the value of n_c can be lowered significantly from the prediction $n_c = 1.28 \pm 0.05$ in the SM to $n_c = 1.23 \pm 0.05$, 1.18 ± 0.05 for $M_{H^+} = 200,100$ GeV, respectively.

In short, the predicted n_c and the measured n_c now agree within roughly one standard deviation after taking into account the effects of gluonic charged Higgs penguin diagrams in the model III with a relatively light charged Higgs boson, while the agreement between the theoretical prediction and the data for B_{SL} can also be improved by inclusion of these new physics effects.

APPENDIX: RS INDEPENDENT $\Delta\bar{\Gamma}_{cc}$, $\Delta\bar{\Gamma}_{peng}$, AND $\Delta\bar{\Gamma}_W$

For the convenience of the reader, we here present the explicit expressions of the RS independent NLO corrections $\Delta\bar{\Gamma}_{cc}$, $\Delta\bar{\Gamma}_{peng}$, and $\Delta\bar{\Gamma}_W$. For more details one can see the original paper [6].

The term $\Delta\bar{\Gamma}_{cc}$ in Eq. (44) describes the current-current type corrections proportional to $C_{1,2}^{(0)}C_{1,2}^{(0)}$ [6]

$$\Delta\bar{\Gamma}_{cc} = t\frac{G_F^2 m_b^5}{32\pi^3}|v_u|^2 \sum_{i,j=1}^{2} C_i^{(0)}C_j^{(0)}\left[h_{ij} + \sum_{k=1}^{2} J_{ki}b_{kj}\right]$$
(A1)

with $t = 1$ for $q = u$ and $t = 0$ for $q = d,s$, and the coefficients h_{ij} and J_{ki} can be found in Ref. [6].

The term $\Delta\bar{\Gamma}_{peng}$ in Eq. (44) describes the effect of penguin diagrams involving $Q_{1,2}$ [6],

$$\Delta\bar{\Gamma}_{peng} = \frac{G_F^2 m_b^5}{32\pi^3}\text{Re}\left[t\sum_{i,j=1,2} C_i^{(0)}C_j^{(0)} v_u \right.$$
$$\times [v_c^* g_{ij}(x_c) + v_u^* g_{ij}(0)]$$
$$\left. - \sum_{\substack{i=1,2 \\ j=3,\ldots 6}} C_i^{(0)}C_j^{(0)} v_t [v_c^* g_{ij}(x_c) + v_u^* g_{ij}(0)] \right]$$
$$+ \text{Re}\left[-t v_u v_t^* \sum_{\substack{i,j=1,2 \\ k=3,\ldots 6}} C_i^{(0)}C_j^{(0)} J_{ki}b_{jk} \right.$$
$$\left. + |\xi_t|^2 \sum_{\substack{i=1,2 \\ j,k=3,\ldots 6}} C_i^{(0)}C_j^{(0)} J_{ki}b_{jk} \right].$$
(A2)

with $t = 1$ for $q = u$ and $t = 0$ for $q = d,s$. The explicit expressions of coefficients g_{ij} and J_{ki} can be found in Ref. [6].

Finally, $\Delta\bar{\Gamma}_W$ is given by

$$\Delta\bar{\Gamma}_W = \frac{G_F^2 m_b^5}{32\pi^3}\left[t\sum_{i,j=1}^{2} |v_u|^2 [C_i^{(0)}\bar{C}_j^{(1)}]b_{ij} \right.$$
$$+ \sum_{i,j=3}^{6} |v_t|^2 [C_i^{(0)}\bar{C}_j^{(1)}]b_{ij}$$
$$\left. - t\sum_{\substack{i=1,2 \\ j=3,\ldots,6}} [C_i^{(0)}\bar{C}_j^{(1)} + \bar{C}_i^{(1)}C_j^{(0)}]\text{Re}(v_u^* v_t) b_{ij} \right].$$
(A3)

where $t = 1$ for $q = u$ and $t = 0$ for $q = d,s$, the b_{ij} have been given in Eq. (51).

[1] *The BaBar Physics Book*, BaBar Collaboration, SLAC Report No. SLAC-R 504, 1998; F. Takasaki, hep-ex/9912004; P. Eerola, Mod. Phys. Lett. A **15**, 185 (2000); Nucl. Instrum. Methods Phys. Res. A **446**, 384 (2000); **446**, 407 (2000).

[2] J. Ellis, hep-ph/9910404; Y.F. Zhou and Y.L. Wu, Mod. Phys. Lett. A **15**, 185 (2000); X.G. He, hep-ph/0001313; C.D. Lü, hep-ph/0001321.

[3] D.S. Du and M.Z. Yang, J. Phys. G **24**, 2009 (1998); C.S. Huang, W. Liao, and Q.S. Yan, Phys. Rev. D **59**, 011701 (1999); D. Atwood and A. Soni, *ibid.* **59**, 013007 (1999); A. Ali, G. Kramer, and C.D. Lü, *ibid.* **59**, 014005 (1999); J. Charles, *ibid.* **59**, 054007 (1999); L.B. Guo, L.S. Liu, and D.S. Du, J. Phys. G **25**, 1 (1999); Y.L. Wu, Chin. Phys. Lett. **16**, 339 (1999); Y.H. Chen, H.Y. Cheng, B. Tseng, and K.C. Yang, Phys. Rev. D **60**, 094014 (1999); X.G. He, C.L. Hsueh, and J.Q. Shi, Phys. Rev. Lett. **84**, 18 (2000).

[4] A. J. Buras and R. Fleischer, in *Heavy Flavor II*, edited by A.J. Buras and M. Lindner (World Scientific, Singapore, 1998), p. 65; G. Buchalla, A.J. Buras, and M.E. Lautenbacher, Rev. Mod. Phys. **68**, 1125 (1996).

[5] R. Fleischer, Z. Phys. C **58**, 483 (1993).

[6] A. Lenz, U. Nierste, and G. Ostermaier, Phys. Rev. D **56**, 7228 (1997).

[7] M. Ciuchini, E. Franco, G. Martinelli, L. Reina, and L. Silverstrini, Phys. Lett. B **344**, 137 (1994); C.S. Gao, C.D. Lü, and Z.M. Qiu, Z. Phys. C **69**, 113 (1995).

[8] K. Chetyrkin, M. Misiak, and M. Munz, Phys. Lett. B **400**, 206 (1997); **425**, 414(E) (1998); M. Ciuchini, G. Degrassi, P. Gabino, and M. Neubert, Nucl. Phys. **B527**, 21 (1998); A.K. Kagan and M. Neubert, Eur. Phys. J. C **7**, 5 (1999).

[9] CLEO Collaboration, S. Ahmed *et al.*, CLEO COF 99-10, hep-ex/9908022.

[10] S. Glashow and S. Weinberg, Phys. Rev. D **15**, 1958 (1977); F.M. Borzumati and C. Greub, *ibid.* **58**, 074004 (1998); *ibid.* **59**, 057501 (1999).

[11] M. Misiak, S. Pokorski and J. Rosiek, in *Heavy Flavor II*, edited by A.J. Buras and M. Lindner (World Scientific, Singapore, 1998).

[12] S. Weinberg, Phys. Rev. D **19**, 1277 (1979); L. Susskind, *ibid.* **20**, 2619 (1979); C.D. Lü and Z.J. Xiao, *ibid.* **53**, 2529 (1996); B. Balaji, *ibid.* **53**, 1699 (1996); G.R. Lu *et al.*, *ibid.* **54**, 5647 (1996); G.R. Lu, Z.H. Xiong, and Y.G. Cao, Nucl. Phys. **B487**, 43 (1997); Z.J. Xiao *et al.*, Chin. Phys. Lett. **16**, 88 (1999); Z.J. Xiao *et al.*, Eur. Phys. J. C **7**, 487 (1999); Z.J. Xiao *et al.*, Commun. Theor. Phys. **33**, 269 (2000).

[13] J.L. Cortes, X.Y. Pham, and A. Tounsi, Phys. Rev. D **25**, 188 (1982); G. Altarelli and S. Petrarca, Phys. Lett. B **261**, 303 (1991); I.I. Bigi, B. Blok, M.A. Shifman, and A. Vainstein, *ibid.* **323**, 408 (1994); A.F. Falk, M.B. Wise, and I. Duniets, Phys. Rev. D **51**, 1183 (1995); J.D. Richman and P.R. Burchat, Rev. Mod. Phys. **67**, 893 (1995).

[14] CLEO Collaboration, B. Barish *et al.*, Phys. Rev. Lett. **76**, 1570 (1996).

[15] Particle Data Group, C. Caso *et al.*, Eur. Phys. J. C **3**, 1 (1998).

[16] E. Bagan, P. Ball, V.M. Braun, and P. Gosdzinsky, Nucl. Phys. **B432**, 3 (1994); E. Bagan, P. Ball, V.M. Braun, and P. Gosdzinsky, Phys. Lett. B **342**, 362 (1995); **374**, 363(E) (1996); E. Bagan, P. Ball, B. Fiol, and P. Gosdzinsky, *ibid.* **351**, 546 (1995).

[17] M. Neubert and C.T. Sachrajda, Nucl. Phys. **B483**, 339 (1997); M. Neubert, hep-ph/0001334, and references therein.

[18] H. Yamamoto, hep-ph/9912308, and references therein.

[19] A. Kagan, Proceedings of the Seventh International Symposium on Heavy Flavor Physics, Santa Barbara CA, 1997, hep-ph/9806266.

[20] CLEO Collaboration, L. Gibbons *et al.*, Phys. Rev. D **56**, 3783 (1997).

[21] CLEO Collaboration, T.E. Browder *et al.*, Phys. Rev. Lett. **81**, 1786 (1998).

[22] D. Atwood and A. Soni, Phys. Lett. B **405**, 150 (1997); H. Fritzsch, *ibid.* **415**, 83 (1997); A. Datta, X.-G. He, and S. Pakvasa, *ibid.* **419**, 369 (1997); F. Yuan and K.T. Chao, Phys. Rev. D **56**, R2495 (1997); D.S. Du, C.S. Kim, and Y.D. Yang, Phys. Lett. B **426**, 133 (1998); I. Halperin and A. Zhitnisky, Phys. Rev. Lett. **80**, 438 (1998); J.L. Rosner, Phys. Rev. D **60**, 074029 (1999).

[23] W.S. Hou and B. Tseng, Phys. Rev. Lett. **80**, 434 (1998); A.L. Kagan and A.A. Petrov, hep-ph/9707354; G.R. Lu, Z.J. Xiao, H.K. Guo, and L.X. Lü, J. Phys. G **25**, L85 (1999).

[24] Z.J. Xiao, C.S. Li, and K.T. Chao, Phys. Lett. B **473**, 148 (2000).

[25] T.P. Cheng and M. Sher, Phys. Rev. D **35**, 3484 (1987); M. Sher and Y. Yuan, *ibid.* **44**, 1461 (1991); W.S. Hou, Phys. Lett. B **296**, 179 (1992); A. Antaramian, L.J. Hall, and A. Rasin, Phys. Rev. Lett. **69**, 1871 (1992); L.J. Hall and S. Winberg, Phys. Rev. D **48**, R979 (1993); D. Chang, W.S. Hou, and W.Y. Keung, *ibid.* **48**, 217 (1993); Y.L. Wu and L. Wolfenstein, Phys. Rev. Lett. **73**, 1762 (1994); D. Atwood, L. Reina, and A. Soni, *ibid.* **75**, 3800 (1995).

[26] D. Atwood, L. Reina, and A. Soni, Phys. Rev. D **55**, 3156 (1997).

[27] C.Q. Geng, P. Turcotte, and W.S. Hou, Phys. Lett. B **339**, 137 (1994).

[28] M. Kabayashi and T. Maskawa, Prog. Theor. Phys. **49**, 652 (1973).

[29] W.S. Hou and R.S. Willey, Phys. Lett. B **202**, 59 (1988); S. Bertolini *et al.*, Nucl. Phys. **B353**, 591 (1991); C.D. Lü, *ibid.* **B441**, 33 (1994).

[30] F.M. Borzumati and C. Greub, Phys. Rev. D **58**, 074004 (1998); **59**, 057501 (1999) (Addendum).

[31] D. Atwood, L. Reina, and A. Soni, Phys. Rev. D **54**, 3296 (1996).

[32] T.M. Aliev and E.O. Iltan, J. Phys. G **25**, 989 (1999).

[33] D. Bowser-Chao, K. Cheung, and W.Y. Keung, Phys. Rev. D **59**, 115006 (1999).

[34] T. Inami and C.S. Lim, Prog. Theor. Phys. **65**, 297 (1981); **65**, 1772(E) (1981).

[35] A.J. Buras, ''Weak Hamiltonian, CP violation and rare decays,'' hep-ph/9806471.

[36] E.Gross, ''Searches for New Physics,'' to be published in the proceedings of EPS-HEP 99, Tampere, Finland, 1999.

[37] N. Cabibbo, G. Gorbó, and L. Maiani, Nucl. Phys. **B155**, 93 (1979).

[38] Y. Nir, Phys. Lett. B **221**, 184 (1989).

[39] C.S. Kim and A.D. Martin, Phys. Lett. B **225**, 186 (1989).

[40] W.S. Hou, R.S. Willey, and A. Soni, Phys. Rev. Lett. **58**, 1608 (1987); W.S. Hou, Nucl. Phys. **B308**, 561 (1988); J.-M. Gérard

and W.S. Hou, Phys. Rev. D **43**, 2909 (1991).

[41] A.J. Buras, M. Jamin, M.E. Lautenbacher, and P.H. Weisz, Nucl. Phys. **B370**, 69 (1992); **B375**, 501 (1992); A.J. Buras, M. Jamin, M.E. Lautenbacher, and P.H. Weisz, *ibid.* **B400**, 37 (1993).

[42] I.I. Bigi, N. Uraltsev, and A. Vainshtein, Phys. Lett. B **293**, 430 (1992); **297**, 477 (1993); B. Blok and M. Shifman, Nucl. Phys. **B399**, 411 (1993); **B399**, 459 (1993).

[43] ALEPH Collaboration, D. Buskulic *et al.*, Phys. Lett. B **359**, 236 (1995).

[44] DELPHI Collaboration, Paper submitted to the HEP'99 Conference, Tampere, Finland, DELPHI 99-111 CONF-298, 1999; DELPHI Collaboration, P. Abreu *et al.*, Phys. Lett. B **426**, 193 (1998).

[45] L3 Collaboration, M. Acciarri *et al.*, Eur. Phys. J. C **13**, 47 (2000).

[46] OPAL Collaboration, G. Abbiendi *et al.*, Eur. Phys. J. C **13**, 225 (2000)

[47] M. Neubert, Phys. Rep. **245**, 259 (1994).